Large Eddy Simulation of turbulent flows around a rotor blade segment using a spectral element method

A. Shishkin and C. Wagner

Abstract Large Eddy Simulations of turbulent flows around a segment of the FX-79-W151 rotor blade have been performed for the Reynolds numbers $Re = 5 \cdot 10^3$ and $Re = 5 \cdot 10^4$ and the angle of attack 12° using a spectral element method with 8th order polynomials. The turbulence statistics obtained in the LES reveal regions of laminar and turbulent flow separation for the lower and higher Reynolds numbers, respectively, which lead to different loads on the blade.

1 Introduction

The presented work was part of a research project aiming at future improvements of wind turbines and particularly at investigating the effect of wind gusts on the rotor blades. The prediction of extreme loads caused by wind gusts is very important for the design of wind turbine blades, but this flow problem can not be accurately simulated based on the Reynolds-Averaged Navier-Stokes (RANS) equations or related numerical methods. In this respect, the Large Eddy Simulation (LES) is a promising technique. Here we present LES results of turbulent flows around a segment of the FX-79-W151 rotor blade with an angle of attack $\alpha = 12^\circ$ for freestream Reynolds numbers $Re = 5 \cdot 10^3$ and $Re = 5 \cdot 10^4$.

The computational domain is shown in Fig.1 (left) and the hybrid structured/unstructured mesh consists of 2116 2D-elements (see Fig.1, right) with 64 Fourier planes in spanwise direction. The boundary conditions are time-independent laminar inflow and periodicity in spanwise direction. Further, the outflow boundary is realized with a sponge zone to damp the vortical structures before they leave the domain.

A. Shishkin and C.Wagner
Institute for Aerodynamics and Flow Technology, DLR – German Aerospace Center, Bunsenstr. 10, 37073 Göttingen, Germany e-mail: Andrei.Shishkin@dlr.de and Claus.Wagner@dlr.de

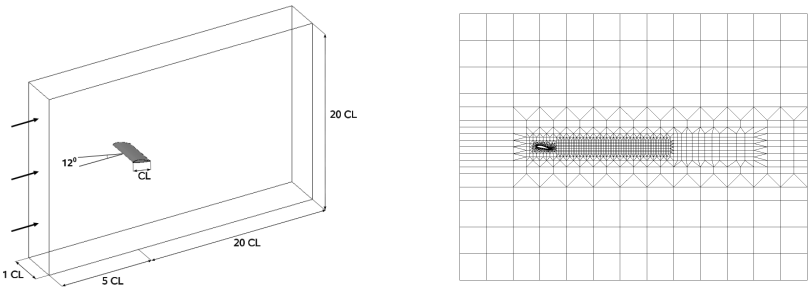

Fig. 1 Schematic view of the computational domain (left) and unstructured 2D mesh (right).

The used SEM is based on polynomial representation of the solution combined with the Fourier extension in homogenous spanwise direction. The temporal discretization is achieved by means of a higher than second order accurate splitting scheme by Karniadakis *et al.* [1]. For the dimensionless Navier-Stokes equations

$$\nabla \cdot \mathbf{u} = 0, \quad \frac{\partial \mathbf{u}}{\partial t} + N(\mathbf{u}) = -\nabla p + L(\mathbf{u}),$$

where $L(\mathbf{u})$ and $N(\mathbf{u})$ denote the linear and non-linear parts of momentum equation, respectively, the following three-step algorithm is used. First, the nonlinear term with the time derivative $\frac{\mathbf{u}^* - \mathbf{u}^n}{\Delta t} = N(\mathbf{u}^n)$ is treated explicitly, then the pressure equation with enforcing the continuity condition $\nabla^2 p^{n+1} = \nabla \cdot \frac{\mathbf{u}^*}{\Delta t}$ is solved, and in the last step the diffusive term $\frac{\mathbf{u}^{n+1} - \mathbf{u}^*}{\Delta t} = -\nabla p^{n+1} + L(\mathbf{u}^{n+1})$ is treated implicitly. Additionly, Adams-Bashforth/Adams-Moulton schemes are used. Further details on the splitting scheme can be found in [1, 2]. We use also the SEM-adapted Smagorinsky subgrid scale model as proposed by Karamanos [3].

2 Results of LES for $Re = 5 \cdot 10^3$ and $Re = 5 \cdot 10^4$

The LES were performed with polynomials of order $N = 8$ (spatial discretization) and a time step $\Delta t = 5 \cdot 10^{-6}$. The predicted flow fields were averaged over 2.5 time units and over the spanwise length to provide the turbulence statistics.

The mean streamwise velocity components depicted in Fig. 2 reflect the flow acceleration over the leading edge and the backflow regions (flow separation) on the suction side (highlighted with white curves) for both Reynolds numbers. Considering the Turbulent Kinetic Energy (TKE) (Fig. 3) it is observed that the area of higher TKE is located downstream the trailing edge for $Re = 5 \cdot 10^3$ (Fig.3, left), while the higher TKE values are located in the suction side area close to the trailing edge for the higher Reynolds number (Fig. 3, right). The mean pressure coefficients are shown in Fig. 4. The local minimum of the pressure coefficient on the suction side close to the trailing edge observed for the higher Reynolds number (Fig. 4, right) indicates a turbulent flow, while the separation region is laminar for the lower

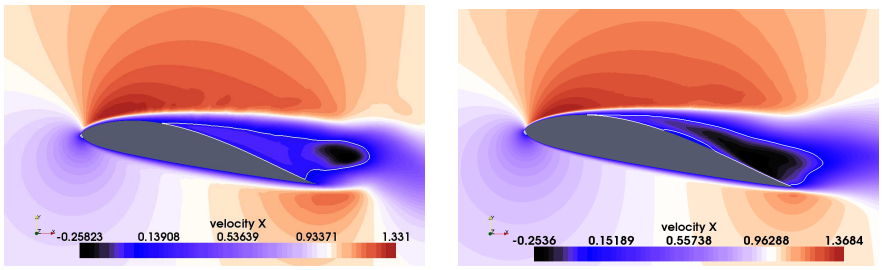

Fig. 2 The mean streamwise velocity components as obtained in the LES for $Re = 5 \cdot 10^3$ (left) and for $Re = 5 \cdot 10^4$ (right). The regions of negative mean velocity (backflow) are outlined.

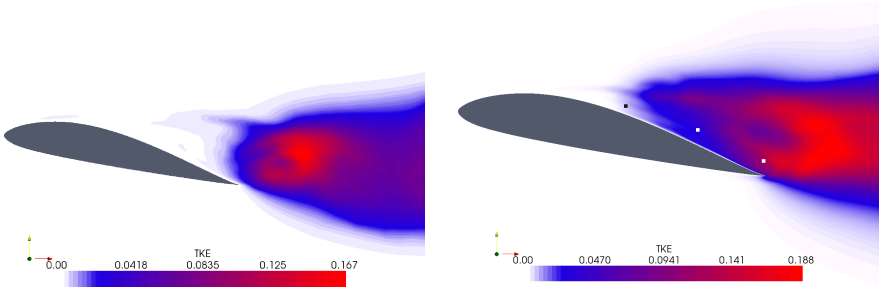

Fig. 3 Distribution of the turbulent kinetic energy obtained in the LES for $Re = 5 \cdot 10^3$ (left) and $Re = 5 \cdot 10^4$ (right).

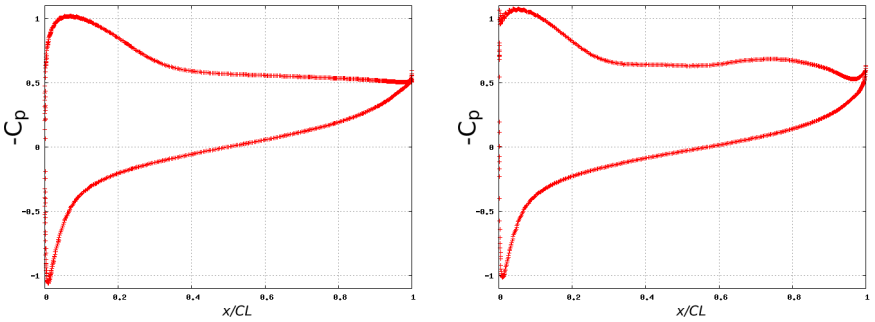

Fig. 4 Mean pressure coefficient obtained in the LES for $Re = 5 \cdot 10^3$ (left) and $Re = 5 \cdot 10^4$ (right).

Reynolds number (Fig. 4, left). Finally, the spatial energy spectras at three locations over the suction side marked in Fig.3 (right) are presented in Fig. 5. Energy spectras taken in the region with higher TKE values (Fig. 5, middle and right top and right bottom) reflect a decay which partly agrees with the ”-5/3” law of isotropic turbulence, while the spectras taken at the other locations are characterized by low energy values and faster decay for all velocity components.

The LES results reflect flow separation and complex flow structures in the vicinity of a rotor blade. The analysis of the flow fields also shows that turbulent separation is observed for the higher Reynolds number while the separation is laminar for the lower one.

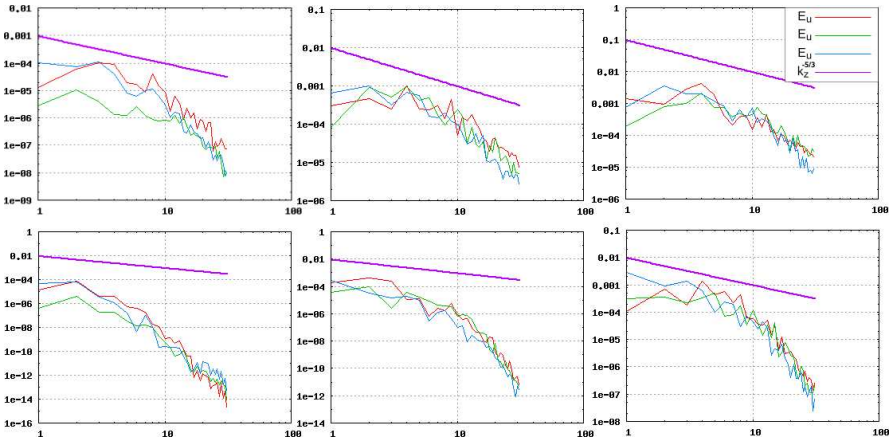

Fig. 5 Energy spectra components for $Re = 5 \cdot 10^4$ (top) and $Re = 5 \cdot 10^3$ (bottom) at the three positions above the trailing edge in Fig. 3.

The computational expense of the SEM (the memory usage is 16G for $5.7 \cdot 10^6$ degrees of freedom; 5.5 CPU seconds are needed for one time step on 32 AMD Opteron 1.7GHz processors) seems to be affordable on modern cluster systems. Earlier, in [4] we used a "full 3D" SEM to conduct Direct Numerical Simulations of turbulent pipe flow. Although a direct comparison of the SEM performance in [4] to the here used "2D+Fourier" version is not possible (the former uses an iterative solver, while a direct one is applied in the latter) we want to emphasize that the computational requirements of the here used SEM is much lower.

Thus, we conclude that the SEM can be applied effectively for LES of turbulent flows in computational domains of moderate complexity.

Acknowledgments

We are grateful to S. Sherwin for providing the SEM code and to the BMBF for financing the project.

References

1. G.E. Karniadakis, M. Israeli and S.A. Orszag (1991). High-order splitting methods for incompressible Navier-Stokes equations, *J. Comp. Phys.*, v.97, 414-443.
2. Karniadakis, G.E. , Sherwin, S. (1999). Spectral/HP Element Methods for CFD. *Oxford University Press,* Oxford.
3. Karamanos, G.-S.(1999) Large Eddy Simulation Using Unstructured Spectral/hp Elements. PhD Thesis, Imperial College.
4. Shishkin, A., Wagner. C. (2006). Direct Numerical Simulation of a turbulent flow using a spectral/hp element method. *Notes on Numer. Fluid Mech.*, v.92, 405-412, Springer, Germany.